Hybrid Materials

DOI: 10.1002/ange.201300440

Ligand-Directed Control over Crystal Structures of Inorganic–Organic Frameworks and Formation of Solid Solutions**

*Hamish H.-M. Yeung, Wei Li, Paul J. Saines, Thomas K. J. Köster, Clare P. Grey, and Anthony K. Cheetham**

The diversity of chemical and physical properties exhibited by inorganic–organic frameworks has led to intense investigation for many applications. Control of structure remains a central element for the optimization of properties such as gas storage, separations, catalysis, magnetism, luminescence, and conductivity.[1] Pore size, framework connectivity and dimensionality can be tailored by variations in the metal nodes and organic linkers.[2] Further control of pore shape and chemistry has recently been achieved by placing ligands with different functional groups on the same crystallographic site in a single phase,[3] thereby enabling improved gas separation,[3c,d] catalysis,[3a] and drug release.[3b] This development is analogous to established solid solutions in important inorganic materials such as ferroelectrics,[4] phosphors,[5] and catalysts.[6] In inorganic–organic frameworks, however, control over stoichiometry, phase segregation, and homogeneity remains a challenge owing to crystallization kinetics, while differentiation between compositions by X-ray diffraction has been limited by the small variations in cell parameters that are found in stable mixed-ligand phases.[3c]

We report herein a new family of isostructural lithium-based inorganic–organic frameworks, which form solid solutions through mechanosynthesis, both in one-step reactions and by combination of the end-member materials. By using high-resolution synchrotron powder X-ray diffraction[7] and cross-polarization solid-state NMR spectroscopy,[8] we demonstrate apparently complete ligand mixing in the resulting binary and ternary systems. Substitution of the ligands results in changes of the unit cell volume of up to 8%, although remarkably, the frameworks have 3D connectivity and contain no solvent-accessible volume. Examination of the single-crystal structures and mechanical properties of the parent compounds reveals that this compositional flexibility is a result of structural flexibility in the metal coordination sphere and ligand conformation.

The family of inorganic–organic frameworks with 3D Li–O–Li connectivity, $\{Li_2(flu)\}_n$ (**1**; flu = tetrafluorosuccinate), $\{Li_2(mal)\}_n$ (**2**; mal = L-malate), $\{Li_2(met)\}_n$ (**3**; met = methylsuccinate), and $\{Li_2(suc)\}_n$ (**4**; suc = succinate), were prepared by solution crystallization of lithium salts with the corresponding ligand (see the Supporting Information for details). Single-crystal X-ray diffraction studies showed that **1**–**3** are isostructural with **4**, which adopts space group $R\bar{3}$[9] (here redetermined at 120 K; Figure 1).[10]

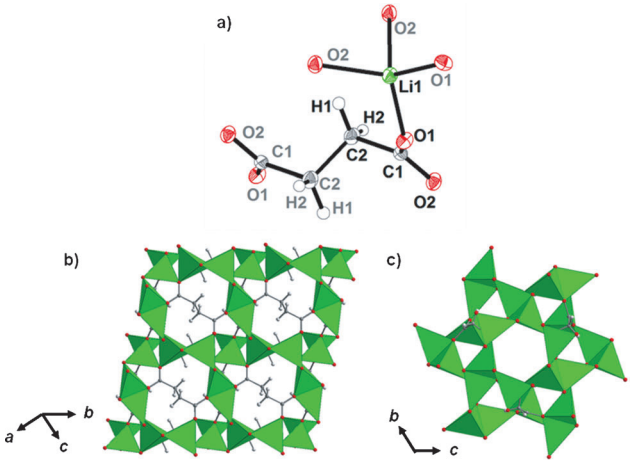

Figure 1. a) ORTEP extended asymmetric unit of **4**; thermal ellipsoids are set at 50% probability for C, Li, and O, and at 20% for H. b, c) The bulk structure showing C, H, and O atoms and LiO_4 tetrahedra in gray, white, red, and green, respectively.

The ligand substituents in **1**–**3** are accommodated by distortions in the unit cell and atomic arrangement of the parent compound **4** (Table 1). Substitution of all alkyl hydrogen atoms by F atoms in **1** causes weakening of Li–O bonds and a reduction in the Li bond valence sum (BVS),[11] owing to electron withdrawal from the carboxylate groups, thereby resulting in expansion of LiO_4 tetrahedra and an increase in the cell volume (V) and the cell parameter ratio (a:c). Fluorination has also been shown to cause the torsion angle between carboxylate groups and the carbon backbone, δ_{CO_2}, to become perpendicular,[12] but the distortion of angles in the LiO_4 tetrahedron, δ_{tet},[13] is constant within experimental error. In contrast, inter-ligand hydrogen bonding between trimers of OH groups in chiral **2** causes a contraction in the ab plane, thus resulting in a decrease in a:c and V. In this case, the

[*] H. H.-M. Yeung, Dr. W. Li, Prof. A. K. Cheetham
Department of Materials Science and Metallurgy
Cambridge University
Pembroke Street, Cambridge, CB2 3QZ (UK)
E-mail: akc30@cam.ac.uk
Dr. P. J. Saines
Inorganic Chemistry Laboratory, Oxford University
South Parks Road, Oxford, OX1 3QR (UK)
Dr. T. K. J. Köster, Prof. C. P. Grey
Department of Chemistry, Cambridge University
Lensfield Road, Cambridge, CB2 1EW (UK)

[**] This work was supported by the EPSRC (research studentship to H.Y.) and ERC (Advanced Investigator Award to A.K.C.). We would like to thank Prof. Chiu Tang for assistance on beamline I11 at Diamond Light Source (UK).

Supporting information for this article is available on the WWW under http://dx.doi.org/10.1002/anie.201300440.

Table 1: Structural distortions and changes in unit cell parameters (**1**, **3**, and **4** in space group $R\bar{3}$; **2** in $R3$) at 120 K in **1**–**4**.

	1	**2**	**3**	**4**
Subst.	4×F	OH	CH_3	H
V [Å^{-3}]	1418.3(10)	1309.5(2)	1375.8(3)	1332.03(14)
a:c	1.17241(6)	1.10801(15)	1.1226(2)	1.14040(9)
Li BVS	0.99	1.09, 1.09	1.02	1.09
δ_{CO_2} [°]	89.9(2)	93.5(3), 73.1(3)	63.8(10)	91.75(14)
δ_{tet} [°]	12.9(9)	10.9(15), 10(2)	11.1(11)	10.9(6)

carboxylate group furthest from the OH group of major occupancy twists, while the Li BVS and δ_{tet} remain the same. The bulky, hydrophobic methyl substituent in **3**, which underwent in situ racemization, causes large amounts of strain, both in V and in the atomic structure. The observation that crystals of the equivalent chiral structure do not form, suggests that the steric interaction between neighboring methyl groups is reduced when a mixture of enantiomeric forms is present.

Compounds **1**, **2**, and **4** formed large, well-defined single crystals, which allowed detailed investigation of the mechanical properties by nanoindentation (Table 2; see Figures S1–S6 in the Supporting Information). Values for the Young's modulus (E) and hardness (H) of {0,1,-1} facets correlate well with packing index, thus indicating that short-range interligand interactions are important for reducing mechanical compliance in these materials. In contrast, values for the directional yield stress (σ_y) correlate with framework bonding: longer Li–O bonds in **1** are broken more easily than those in **2** and **4**, thereby resulting in the lowest σ_y value. **2** and **4** have similar Li–O bond strengths, but the additional hydrogen bonding between ligands in **2** causes an increase in its σ_y value. While **1**, **2**, and **4** exhibit negligible creep owing to their 3D Li–O–Li network, they are more compliant than most nonporous inorganic–organic frameworks previously studied.[14] The ionic lithium coordination sphere and torsional degrees of freedom associated with the succinate-based ligands impart more flexibility than, for example, covalent copper-based units[15] and rigid oxalate ligands.[16]

Table 2: Mechanical properties measured by nanoindentation and calculated packing indices of **1**, **2**, and **4**.

	1	**2**	**4**
Substituent	4×F	OH	H
Packing index[a] [%]	82.7	79.8	73.5
Young's modulus, E [GPa]	33.2(10)	29.8(7)	20.3(6)
Hardness, H [GPa]	2.35(7)	2.28(6)	1.65(6)
Yield stress, σ_y [GPa]	0.860(13)	1.62(2)	1.116(15)

[a] Calculated by using PLATON;[17] only the moiety of the disordered ligand with major occupancy in **2** was considered.

The flexibility, both compositional and structural, of this family of compounds suggested that it could be possible to synthesize mixed-ligand phases with continuous variation in properties between two or more pure end members. Mechanochemistry has recently been employed by our group both in the synthesis[18] and amorphization[19] of zeolitic imidazolate frameworks. In addition, Adams et al.[20] showed that it offers fine control of the cell metrics of perhalocobalt bipy (bipy = 4,4′-bipyridine) coordination polymers through variation of the Cl:Br ligand ratio. In this work, we believe that the solvent-free conditions[21] and constant disruption of particulates in the grinding process enable kinetic stabilization of homogeneous mixed-ligand phases. This may be contrasted with the high temperatures used in the synthesis of inorganic solid solutions; these temperatures prevent phase separation by raising the entropic contribution to free energy, $T\Delta S$, but are not compatible with inorganic–organic framework materials owing to their lower stability.

The binary solid solution $\{Li_2(suc)_{1-x}(flu)_x\}_n$ (denoted as **4·1** (x), where $x = 0$–1) and the ternary system $\{Li_2(suc)_x(mal)_y(met)_z\}_n$ (denoted as **4·2·3** (x:y:z), where $x+y+z=1$) were synthesized by grinding stoichiometric amounts of the component precursors for 30 min (see the Supporting Information for details). High-resolution synchrotron powder X-ray diffraction (HRS-PXRD) data were obtained for **4·1** in stepwise increments of x, showing large shifts in cell parameters (Figure 2). Rietveld refinement gave accurate cell parameters for each sample and fractional occupancies for H and F atoms consistent with elemental analysis and the reagent stoichiometry (see Figures S7–S8, S13–S14). V varies linearly with x, thus obeying Vegard's law.[22] Cell parameters a and c vary nonlinearly (Figure 3), thereby demonstrating anisotropic structural strain owing to ligand mixing. The HRS-PXRD data reveal some peak broadening in the solid solutions compared with the end members, not observable in laboratory data. This could simply be due to local strain effects, or it might reflect a slightly inhomogeneous distribution of the ligand within individual particles.

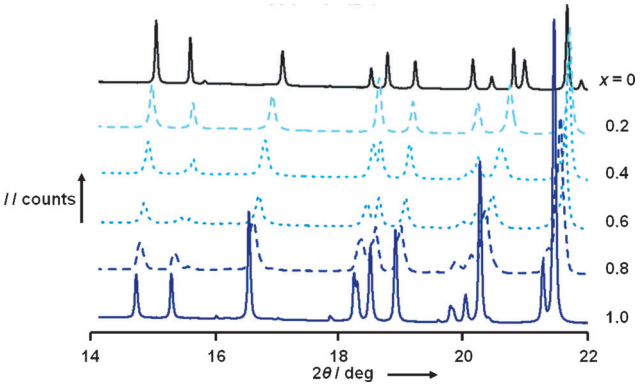

Figure 2. HRS-PXRD data for the binary solid solution $\{Li_2(suc)_{1-x}(flu)_x\}_n$ (**4·1** (x = 0–1); λ = 0.826124 Å).

^{13}C–^{1}H cross-polarization (CP) solid-state MAS-NMR spectroscopy was used to confirm ligand mixing in the sample **4·1** (0.5), thereby giving qualitative insight into the spatial proximity of suc and flu ligands. In the CP experiment, the ^{13}C nuclei were polarized indirectly by a magnetization transfer from coupled protons. The two different carbon atoms of suc ligands in **4·1** (0.5) as well as the carboxylate carbon atom in the flu ligand (168 ppm) were observed. Since the flu anion does not contain any protons, the observed signal must be due

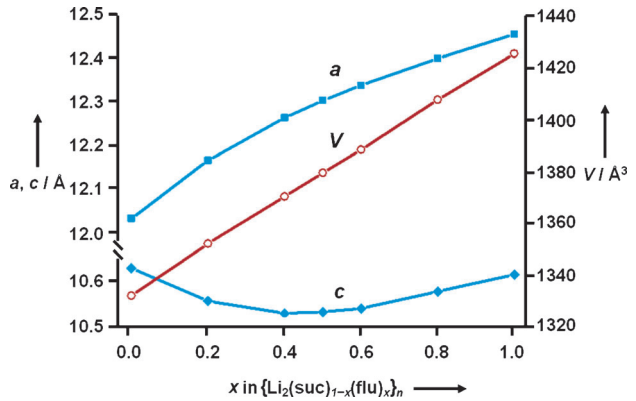

Figure 3. Unit cell parameters for **4·1** ($x = 0$–1) from Rietveld refinement of HRS-PXRD data. Error bars are smaller than markers.

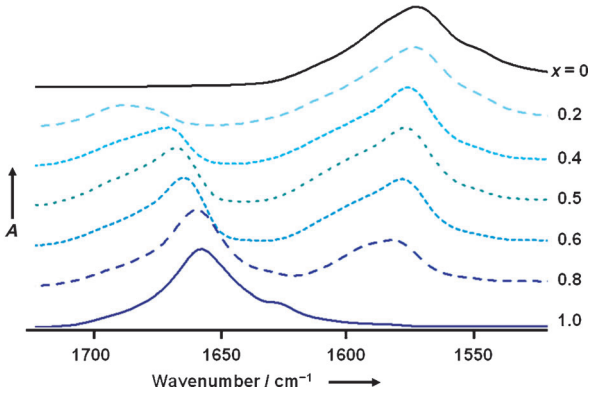

Figure 5. a) FTIR of **4·1** ($x = 0$–1) in the carboxylate region.

to a polarization transfer from suc protons to flu ^{13}C nuclei. The intensity of peaks in the ^{13}C spectrum was measured as a function of cross-polarization contact time; a signal at 168 ppm was observed, which corresponds to flu ^{13}C nuclei excited by protons on nearby suc ligands (Figure 4). The

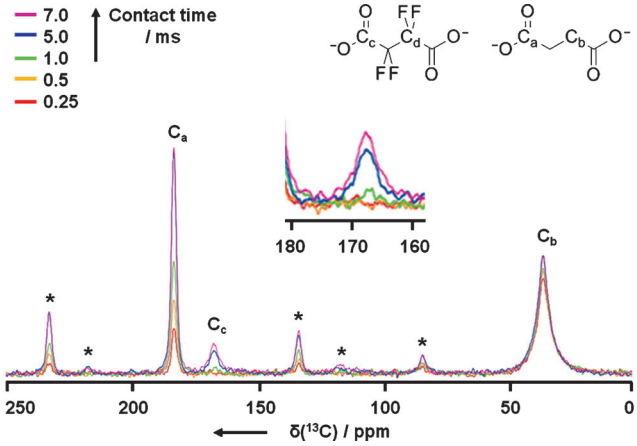

Figure 4. ^{13}C–^{1}H CP MAS-NMR of **4·1** (0.5) with variable contact time. The inset shows the region at 160–180 ppm. C_d is not observed owing to a lack of ^{19}F decoupling; asterisks mark spinning sidebands from C_a and C_c.

build-up of this peak was slower than those of suc nuclei owing to their different distances from suc protons, as expected from the crystallographic structure (see Figures S9, S10 in the Supporting Information). Notably, owing to poor ^{1}H–^{13}C coupling, the ^{13}C–^{1}H CP MAS-NMR spectrum of tetrafluorosuccinic acid contains no peaks (see Figure S11 in the Supporting Information), thus confirming that the flu signal in **4·1** (0.5) arises because of the proximity of the different ligands on the molecular level in the same crystalline phase.

The ratio of peaks from suc and flu ligands in the FTIR spectra of **4·1** varies smoothly with x (Figure 5). As a further indication of ligand mixing, the CO_2^- antisymmetric stretch assigned to one ligand shifts to higher frequency owing to perturbation of the structure as the fraction of the other increases, which forces the suc and flu ligands into progressively larger and smaller coordination environments, respectively. Thermogravimetric analysis (TGA) of **4·1** shows a decrease in decomposition temperature as the ligands are mixed, with **4·1** ($x = 0.8$) having the lowest stability (see Figure S12 in the Supporting Information).

The cell parameters of the ternary system **4·2·3** were determined by Le Bail fitting of HRS-PXRD data. V varies most with increasing z, owing to the steric bulk of methyl substituents, whereas it remains almost unchanged when x and y vary independently of z (Figure 6). The largest stepwise increase in V is seen from **4·2·3** (0:1:0) to (0:0.8:0.2), which is due to the simultaneous disruption of cooperative hydrogen bonding and addition of methyl groups to the mal-ligand-rich sample.

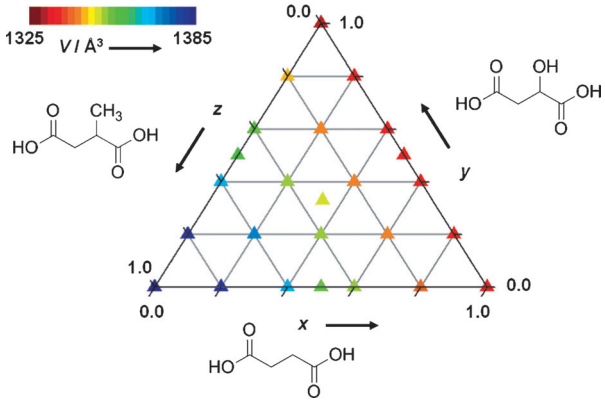

Figure 6. Trends in cell volume (V) of the ternary system **4·2·3** (x:y:z).

In summary, our work represents significant progress in the area of inorganic–organic frameworks for four important reasons. Firstly, through the combination of HRS-PXRD and CP MAS-NMR spectroscopy we demonstrate complete solid solutions in the binary and ternary systems, $\{Li_2(suc)_{1-x}(flu)_x\}_n$ and $\{Li_2(suc)_x(mal)_y(met)_z\}_n$, respectively. Secondly, we present a simple, cheap, and efficient method, namely mechanochemical synthesis, used for the first time to produce mixed-ligand materials. Thirdly, through examination of the single-crystal structures and mechanical properties of the isostruc-

tural parent compounds, we show that this compositional flexibility is a result of structural flexibility in the metal coordination environment and ligand torsional angles. Finally, this work is the first of its kind involving a 3D, dense inorganic–organic framework system, opening up the possibility of similar investigations into materials that were to date thought to be unsuitable for ligand substitution. These materials have potential applications owing to their conducting, ferroelectric, luminescent, and magnetic behavior.[1a,b]

Received: January 17, 2013
Published online: March 26, 2013

Keywords: inorganic–organic frameworks · ligand effects · lithium · nanoindentation · solid solution

[1] a) C. Janiak, *Dalton Trans.* **2003**, 2781 – 2804; b) C. N. R. Rao, A. K. Cheetham, A. Thirumurugan, *J. Phys. Condens. Matter* **2008**, *20*, 083202; c) S. Horike, S. Shimomura, S. Kitagawa, *Nat. Chem.* **2009**, *1*, 695 – 704.

[2] a) M. Eddaoudi, J. Kim, N. Rosi, D. Vodak, J. Wachter, M. O'Keeffe, O. M. Yaghi, *Science* **2002**, *295*, 469 – 472; b) L. N. Appelhans, M. Kosa, A. V. Radha, P. Simoncic, A. Navrotsky, M. Parrinello, A. K. Cheetham, *J. Am. Chem. Soc.* **2009**, *131*, 15375 – 15386; c) P. J. Saines, P. Jain, A. K. Cheetham, *Chem. Sci.* **2011**, *2*, 1929 – 1939; d) P. J. Saines, M. Steinmann, J.-C. Tan, H. H.-M. Yeung, W. Li, P. T. Barton, A. K. Cheetham, *Inorg. Chem.* **2012**, *51*, 11198 – 11209.

[3] a) W. Kleist, F. Jutz, M. Maciejewski, A. Baiker, *Eur. J. Inorg. Chem.* **2009**, 3552 – 3561; b) K. M. L. Taylor-Pashow, J. Della Rocca, Z. G. Xie, S. Tran, W. B. Lin, *J. Am. Chem. Soc.* **2009**, *131*, 14261; c) T. Fukushima, S. Horike, Y. Inubushi, K. Nakagawa, Y Kubota, M. Takata, S. Kitagawa, *Angew. Chem.* **2010**, *122*, 4930 – 4934; *Angew. Chem. Int. Ed.* **2010**, *107*, 19033 – 16038; d) H. X. Deng, C. J. Doonan, H. Furukawa, R. B. Ferreira, J. Towne, C. B. Knobler, B. Wang, O. M. Yaghi, *Science* **2010**, *327*, 846 – 850; e) S. Marx, W. Kleist, J. Huang, M. Maciejewski, A. Baiker, *Dalton Trans.* **2010**, *39*, 3795 – 3798.

[4] G. Catalan, J. F. Scott, *Adv. Mater.* **2009**, *21*, 2463 – 2485.

[5] H. A. Höppe, *Angew. Chem.* **2009**, *121*, 3626 – 3636; *Angew. Chem. Int. Ed.* **2009**, *48*, 3572 – 3582.

[6] A. K. Cheetham, G. Férey, T. Loiseau, *Angew. Chem.* **1999**, *111*, 3466 – 3492; *Angew. Chem. Int. Ed.* **1999**, *38*, 3268 – 3292.

[7] S. P. Thompson, J. E. Parer, J. Marchal, J. Potter, A. Birt, F. Yuan, R. D. Fearn, A. R. Lennie, S. R. Street, C. C. Tang, *J. Synchrotron Radiat.* **2011**, *18*, 637 – 648.

[8] H. C. Hoffmann, M. Debowski, P. Müller, S. Paasch, I. Senkovska, S. Kaskel, E. Brunner, *Materials* **2012**, *5*, 2537 – 2572.

[9] H. Klapper, H. Kuppers, *Acta Crystallogr. Sect. B* **1973**, *29*, 21 – 26.

[10] Crystal data for **1** – **4** can be found in the Supporting Information. CCDC 910413, 910414, 910415, 910416 contain the supplementary crystallographic data for this paper. These data can be obtained free of charge from The Cambridge Crystallographic Data Centre via www.ccdc.cam.ac.uk/data_request/cif.

[11] N. E. Brese, M. O'Keeffe, *Acta Crystallogr. Sect. B* **1991**, *47*, 192 – 197.

[12] T. Friščić, D. G. Reid, G. M. Day, M. J. Duer, W. Jones, *Cryst. Growth Des.* **2011**, *11*, 972 – 981.

[13] M. Harding, *Acta Crystallogr. Sect. D* **2000**, *56*, 857 – 867.

[14] J.-C. Tan, A. K. Cheetham, *Chem. Soc. Rev.* **2011**, *40*, 1059 – 1080.

[15] J.-C. Tan, C. A. Merrill, J. B. Orton, A. K. Cheetham, *Acta Mater.* **2009**, *57*, 3481 – 3496.

[16] J.-C. Tan, J. D. Furman, A. K. Cheetham, *J. Am. Chem. Soc.* **2009**, *131*, 14252 – 14254.

[17] A. L. Spek, *Acta Crystallogr. Sect. D* **2009**, *65*, 148 – 155.

[18] P. J. Beldon, L. Fabian, R. S. Stein, A. Thirumurugan, A. K. Cheetham, T. Friščić, *Angew. Chem.* **2010**, *122*, 9834 – 9837; *Angew. Chem. Int. Ed.* **2010**, *49*, 9640 – 9643.

[19] T. D. Bennett, S. Cao, J.-C. Tan, D. A. Keen, E. G. Bithell, P. J. Beldon, T. Friščić, A. K. Cheetham, *J. Am. Chem. Soc.* **2011**, *133*, 14546 – 14549.

[20] C. J. Adams, M. F. Haddow, M. Lusi, A. G. Orpen, *Proc. Natl. Acad. Sci. USA* **2010**, *107*, 16033 – 16038.

[21] Liquid drops of ca. 50 μL and water produced during the reaction are not thought to dissolve reagents enough to be considered solvents.

[22] L. Vegard, *Z. Phys.* **1921**, *5*, 17 – 26.

